Ref.TH.1941-CERN

IMPACT PARAMETER DESCRIPTION OF THE CHARGE EXCHANGE PROCESS $\pi^+p \to \pi^0(\pi^+p)$

J.P. Ader, S. Humble and R. Peschanski
CERN — Geneva

and

R.Lacaze
Université de Genève,
Département de Physique Théorique

ABSTRACT

The "Reggeometry" model - universal impact parameter profile and Regge behaviour - is applied to recent data on $\pi^+p \to \pi^0(p\pi^+)$ at different energies and (π^+p) missing masses, including Δ production. We are able, in particular, to explain the filling of the dips and the variation of the slope with respect to the missing mass.

Ref.TH.1941-CERN
18 October 1974

High energy two-body and quasi-two-body phenomenology has for many years been discussed predominantly in terms of t channel exchanges, in particular Regge poles and absorptive cuts. However, while there is considerable evidence to suggest that Regge pole exchanges may be a good first approximation to the true dynamical situation, it must be admitted that even rather elaborate Regge cut prescriptions cannot yet fully explain all the fine details of the scattering data.

If one looks at these data in terms of s channel dynamics, on the other hand, it has recently been suggested [1),2)] that they may display a systematic structure which is extremely simple. For example, if one takes the impact parameter profile $\tilde{M}_n(b,s)$ of each s channel helicity amplitude $M_n(s,t)$ with net helicity flip n, such that

$$\tilde{M}_n(b,s) = \frac{1}{q^2}\int_0^\infty d(-t')\, J_n(b\sqrt{-t'})\, M_n(s,t') \qquad (1)$$

it has been postulated that there exists a "b universality" which trivially relates these profiles for different values of n. Taking into account the kinematical constraints : $M_n(s,b) = 0(b^n)$ near $b=0$, it was suggested in Ref. 1) that the profiles for all n are given by :

$$\tilde{M}_n(b,s) \propto b^n f(s,b) \qquad (2)$$

where f(s,b) is the same for all helicity amplitudes. Thus, if one knows the structure of one helicity amplitude, one can easily calculate the profiles for each helicity, using Eqs. (1) and (2), and hence determine all the helicity amplitudes from the inverse transform :

$$M_n(s,t') = 2q^2\int_0^\infty db\, b\, J_n(b\sqrt{-t'})\, \tilde{M}_n(b,s) \qquad (3)$$

In fact, from amplitude analyses, etc., it seems that in many cases there is some helicity amplitude $M_{nR}(s,t')$ which can be associated quite closely with a pure Regge pole exchange. Hence it should be possible to use the simple Regge pole parametrization to calculate $\tilde{M}_{nR}(s,b)$ and hence the universal function f(s,b) of Eq. (2), and so determine all other helicity amplitudes. For example, the $\pi^- p \to \pi^0 n$ CEX data strongly suggest that the helicity flip amplitude is predominantly a pure ρ Regge pole exchange, so that we may write

$$M_{n_R=1}(s,t') \propto \sqrt{-t'}\left(\frac{s}{s_0}\right)^{\alpha(t)}\left(1 - e^{-i\pi\alpha(t)}\right) \quad (4)$$

where $\alpha(t) = 0.5 + 0.9t$ and s_0 is a scale parameter. Then inserting Eq. (4) into Eq. (1) and using Eq. (2) to calculate the other profiles, we find that

$$M_n(s,t') = \lambda_n(s)\left(\sqrt{-t'}\right)^n\left[\frac{d}{\sqrt{-t'}\,d\sqrt{-t'}}\right]^{n-1}\left\{\frac{M_1(s,t')}{\sqrt{-t'}}\right\} \quad (5)$$

$$= \lambda_n(s)\left(\sqrt{-t'}\right)^n\left(\frac{s}{s_0}\right)^{\alpha(t)}\left\{\left[\alpha' \log\left(\frac{s}{s_0}\right)\right]^{n-1} - e^{-i\pi\alpha}\left[\alpha'\left(\log\left(\frac{s}{s_0}\right) - i\pi\right)\right]^{n-1}\right\}$$

where $\lambda_n(s)$ are in principle arbitrary. However, from Eq. (5) we see that each helicity amplitude goes like $\lambda_n(s)(\log s/s_0)^{n-1}(s/s_0)^{\alpha(t)}$ at large s. Therefore it is convenient to choose $\lambda_n(s)$ to have the symmetric form

$$\lambda_n(s) = \lambda_n\left\{\frac{1}{2}\left[\log\left(\frac{s}{s_1}\right) + \log\left(-\frac{s}{s_1}\right)\right]\right\}^{1-n}$$

$$= \lambda_n\left[\log\left(\frac{s}{s_1}\right) - i\frac{\pi}{2}\right]^{1-n} \quad (6)$$

so that <u>each</u> helicity amplitude behaves like a dominant Regge pole (+ Regge cuts) at sufficiently large s. Notice that in Eq. (5) only $M_1(s,t')$ is a Regge pole amplitude. All other amplitudes are modified to some extent (i.e., have absorptive cut corrections) but in a very definite and prescribed way.

In Ref. 1) these two basic assumptions of b universality and Regge pole dominance of $M_{nR}(s,t')$ - under the title of <u>Reggeometry</u> - were tested on a number of two-body reactions between 6 and 50 GeV/c. On the whole, the results were most impressive, particularly for the vector exchange contributions. In view of this success, it is worth stressing that the Reggeometry assumptions should apply not only to two-body processes, but also to high mass exclusive, inclusive, and semi-inclusive reactions. In the multi-Regge formalism, the scale parameter s_0 is, in a natural way, proportional to the square of the produced mass M_x, at least at large values of M_x^2. Therefore in such reactions the t' dependence of each helicity amplitude is a priori

fully determined. When M_x^2 increases, of course, the spin of the produced system is also likely to increase, and hence also the number of helicity amplitudes. Thus the only remaining parameters are the relative contribution of each helicity amplitude, i.e., the parameters λ_n in Eq. (6).

As an example of this application of Reggeometry to production processes, in this note we report on an analysis of the (vector) charge exchange production process $\pi^+p \to \pi^0(\pi^+p)$ for which interesting data at 8, 16 and 23 GeV/c have recently become available [3].

a) $\underline{\pi^+p \to \pi^0\Delta^{++}}$

For π^+p masses below 1.4 GeV, the reaction is dominated by $\Delta^{++}(1236)$ production. Therefore before discussing the high mass production data, let us consider first this quasi-two-body reaction. From the description of the CEX process $\pi^-p \to \pi^0n$, reported in Ref. 1), the two parameters s_0, s_1 were determined to be

$$s_0 = 0.32 \equiv \bar{s}_0$$
$$s_1 = 0.32 \equiv \bar{s}_1 \qquad (7)$$

From our previous remarks, we might expect that in the $\Delta(1236)$ production process

$$s_0 = \bar{s}_0 \left(\frac{M_x^2}{m_N^2}\right) = 0.55$$
and [*] $$s_1 = \bar{s}_1 \left(\frac{M_x^2}{m_N^2}\right) = 0.55 \qquad (8)$$

In fact, it is found in fitting the $\pi^+p \to \pi^0\Delta^{++}$ differential cross-sections from 5 to 23 GeV/c, shown in Fig. 1 [3)-5)], and the density matrix elements at 5.45 GeV/c shown in Fig. 2 that the optimal value of both s_0 and s_1 is 0.34 not 0.55. However, Eqs. (8) are by no means rigorously determined by Regge theory. For example, if one thinks of the Regge propagator $(s/s_x)^{\alpha(t)}$ as the high energy approximation of $(\cos\theta_t)^{\alpha(t)}$ where θ_t is the t channel scattering angle, then instead of Eq. (8) we have :

---

*) Since s_1 appears in the arbitrary normalization functions $\lambda_n(s)$, it is not essential that s_1 should have the same M_x^2 dependence as s_0. However, it is found to be a very satisfactory, simplifying assumption.

$$s_0 = \bar{s}_0 \frac{\cos \vartheta_t^{\pi N}}{\cos \vartheta_t^{\pi \Delta}} \qquad (9)$$

where $\vartheta^{\pi N}$, $\vartheta^{\pi \Delta}$ refer to the processes $\pi^- p \to \pi^0 n$ and $\pi^+ p \to \pi^0 \Delta^{++}$, respectively. Although this ratio of cosines depends quite strongly on t', it is found that for small t' values Eq. (9) does not approach the simple multi-Regge form of Eq. (8), until $M_x \gtrsim 2m_n$. For smaller values of M_x on the other hand, Eq. (10) tends to give much lower values of s_0 than does Eq. (8) with the same $\bar{s}_0$. We believe therefore that the optimum value of $s_0 = 0.34$ merely reflects a very low mass breakdown of the Regge parametrization used in Eq. (8). In considering the differential cross-sections $d\sigma/dt'$ for the production process as a function of M_x therefore we write

$$\begin{aligned} s_0 &= \bar{s}_0 \; 1.06 \quad , \quad 1.08 < M_x < 1.4 \text{ Gev} \\ &= \bar{s}_0 \; 2.54 \quad , \quad 1.4 < M_x < 1.8 \text{ Gev} \\ &= \bar{s}_0 \; M_x^2/m_N^2 \qquad M_x > 1.8 \text{ Gev} \end{aligned} \qquad (10)$$

and similarly for s_1.

b) $\underline{\pi^+ p \to \pi^0 (\pi^+ p)}$

Let us now extend our discussion to higher M_x masses. Here the data indicate that the dip near $|t'| = 0.6 (\text{GeV}/c)^2$ which is clearly observed in the $\Delta(1236)$ distributions becomes much less pronounced in the higher mass regions. In fitting the $\Delta(1236)$ distributions only two helicity amplitudes $M_0(s,t)$ and $M_1(s,t)$ were required, with the strength parameters λ_0, λ_1 of Eq. (6) in the ratio

$$\lambda_0 / \lambda_1 = -3.68$$

However, it is apparent that even allowing this ratio to vary at each value of M_x, one cannot account for the shape of these $d\sigma/dt'$ distributions in the higher mass regions at all energies simultaneously with only these two amplitudes. This is illustrated in Fig. 3, where the broken curves represent an optimum "fit" to the data at all three energies with the relative strengths of the two helicity amplitudes given in Table 1. Notice that, as in Ref. 3)*), it

*) In Ref. 3), the dual absorption model parametrization of Loos and Matthews [6] was found to describe the $\Delta^{++}(1236)$ data quite well, [see also Ref. 7)]. However, with only $n = 0,1$ amplitudes it was unable to describe adequately the data at higher missing masses.

is found that either the slopes of the distributions tend to too steep and/or the predicted cross-sections at large t' values are too large *).

However, as M_x increases, so will the effective spin of the produced π^+p system and so, it is reasonable to assume, will the helicity of the system. We therefore try to describe these distributions at all three energies by allowing several helicity amplitudes to contribute. The resulting successful fit is indicated by the solid line in Fig. 3 and corresponds to the values of the helicity strength parameters given in Table 2. Notice that as M_x increases, progressively higher helicity flip amplitudes do indeed contribute. However, there is no evidence that the low helicity amplitudes decrease in strength relative to the higher ones. That is to say, once the helicity amplitude has been "switched on", its relative strength does not change. This is just the universal limiting strength hypothesis of Ref. 2). Note also that the intriguing disappearance and then reappearance of the dip near $|t'| = 0.6$ suggested by the data is now readily explained. The dip which is in the $\Delta\lambda = 1$ amplitude tends to be filled in by the addition of higher helicity amplitudes. However, because of the $(t')^{\Delta\lambda/2}$ behaviour of these amplitudes, for sufficiently large values of $\Delta\lambda$ their effect is to produce a bump above $|t'| = 0.6$ which recreates the dip near this point. Furthermore, it is also this addition of more and more helicity amplitudes which reduces the slope of the distributions in the near forward direction as the mass M_x increases. It is worth while to stress that such a feature could not be satisfactorily explained with only the $\Delta\lambda = 0,1$ amplitudes.

Together with b universality, we have used two hypotheses - universal limiting strength and Eq. (10) as variation law of $s_o(M_x^2)$. The lack of accuracy in the data forbids, however, a definite conclusion about these hypotheses, but one may obtain some partial indications. Having tried to fit, for each mass bin, s_o and the different λ_i/λ_o, we can conclude :

a) λ_1/λ_o seems independent of M_x;

b) s_o has to increase with M_x.

As a typical example : releasing the universal limiting strength (see Table 2) and using, instead of (10) the variation law $s_o = 0.34\ M_x^2/M_\Delta^2$, leads to the results of Fig. 3 (dash-dotted curves) for $1.8 \leq M_{\pi^+p} < 2.4$. They are quite comparable to the previous fit and no spectacular improvement is obtained.

---

*) We discount the distributions in the highest mass region of the 8 GeV/c data. A cut has been made in the $\pi^+\pi^o$ mass distribution to remove events corresponding to the process $\pi^+p \to \rho^+p$. At 8 GeV/c the ρ band overlaps very strongly with the high mass π^+p region and a simple mass cut probably grossly distorts the shape and normalization of the CEX distribution.

To conclude, therefore, we believe this success of Reggeometry in describing the momentum transfer distributions of the $\pi^+p \to \pi^0(\pi^+p)$ exclusive process is very significant. We have been able to describe these distributions in terms of helicity amplitudes which are essentially determined from the effective trajectory obtained by πN CEX process. The only free parameters, besides the over-all normalization, are the relative strength parameters which themselves are found to have a rather simple and systematic dependence on the produced mass M_X.

In principle therefore Reggeometry provides us with a description of production processes which, for the first time, allows us to break away from the oversimplified and naïve Regge pole exchange model. Thus Reggeometry clearly has far-reaching implications not only for two-body scattering, but also for the whole phenomenology of production processes.

TABLE 1 - Coupling constants with $\Delta\lambda = 0,1$ $(\sqrt{\mu b}/GeV)$

	$M_x < 1.4$ GeV	$1.4 < M_x < 1.8$	$1.8 < M_x < 2.4$	$2.4 < M_x < 3.4$
λ_o	27.2	13.0	31.5	61.2
λ_1	100	41.7	96.2	79.4

TABLE 2 - Coupling constants with $\Delta\lambda = 0,1,2,3,4$
(solutions without universal limiting strength are given between brackets)

	$M_x < 1.4$ GeV	$1.4 < M_x < 1.8$	$1.8 < M_x < 2.4$	$2.4 < M_x < 3.4$
λ_o	27.2	10.8	27.2	34
λ_1 / λ_o	-3.68	-3.68	-3.68 (-3.68)	-3.68
λ_2 / λ_o	-	2.0	2.0 (3.2)	2.0
λ_3 / λ_o	-	1.7	1.7 (1.6)	1.7
λ_4 / λ_o	-	-	-	1.03

REFERENCES

1) J.P. de Brion and R. Peschanski, CERN preprint TH.1848 (1974), to be published in Nuclear Phys. B;
J.P. Ader et al., "Reggeometry", CERN preprint TH.1903 (1974).

2) S. Humble, Nuclear Phys. B76, 137 (1974) and CERN preprint TH.1920 (1974).

3) M. Deutschmann et al., CERN preprint DPhII/PHYS 74-35 (1974).

4) I.J. Bloodworth et al., paper No.180, Aix-en-Provence Conference (1973).

5) J.N. Scharenguivel et al., Nuclear Phys. B36, 363 (1972).

6) J.S. Loos and J.A.J. Matthews, Phys.Rev. D6, 246 (1972),

7) I.J. Bloodworth, Nuclear Phys. B80, 230 (1974).

* * * * * * * * * * *

FIGURE CAPTIONS

Figure 1 : Differential cross-sections for the process $\pi^+p \to \pi^o\Delta^{++}$ from 5.45 to 23 GeV/c. Data are taken from Refs. 3), 4), 5).

Figure 2 : The density matrix elements for the process $\pi^+p \to \pi^o\Delta^{++}$ at 5.45 GeV/c [Ref. 4)]. The solid curves are the Reggeometry description of the process using $\lambda_o/\lambda_1 = -3.68$ and assuming a value of 0.43 for the ratio $M_{1\,\frac{1}{2}\,\frac{1}{2}}/M_{3\,\frac{1}{2}\,\frac{1}{2}}$.

Figure 3 : $d\sigma/dt'$ distributions for four π^+p mass intervals at 8, 16 and 23 GeV/c. The broken curves are obtained by assuming $\Delta\lambda = 0,1$ contributions only. The solid curves are given by several helicity amplitudes as indicated in Table 2. The dash-dotted curves for the π^+p mass interval (1.8, 2.4 GeV) correspond to a solution violating the USL hypothesis. The distribution for $M(\pi^+p) > 2.4$ GeV in the 8 GeV/c data are disregarded for reasons discussed in the text.

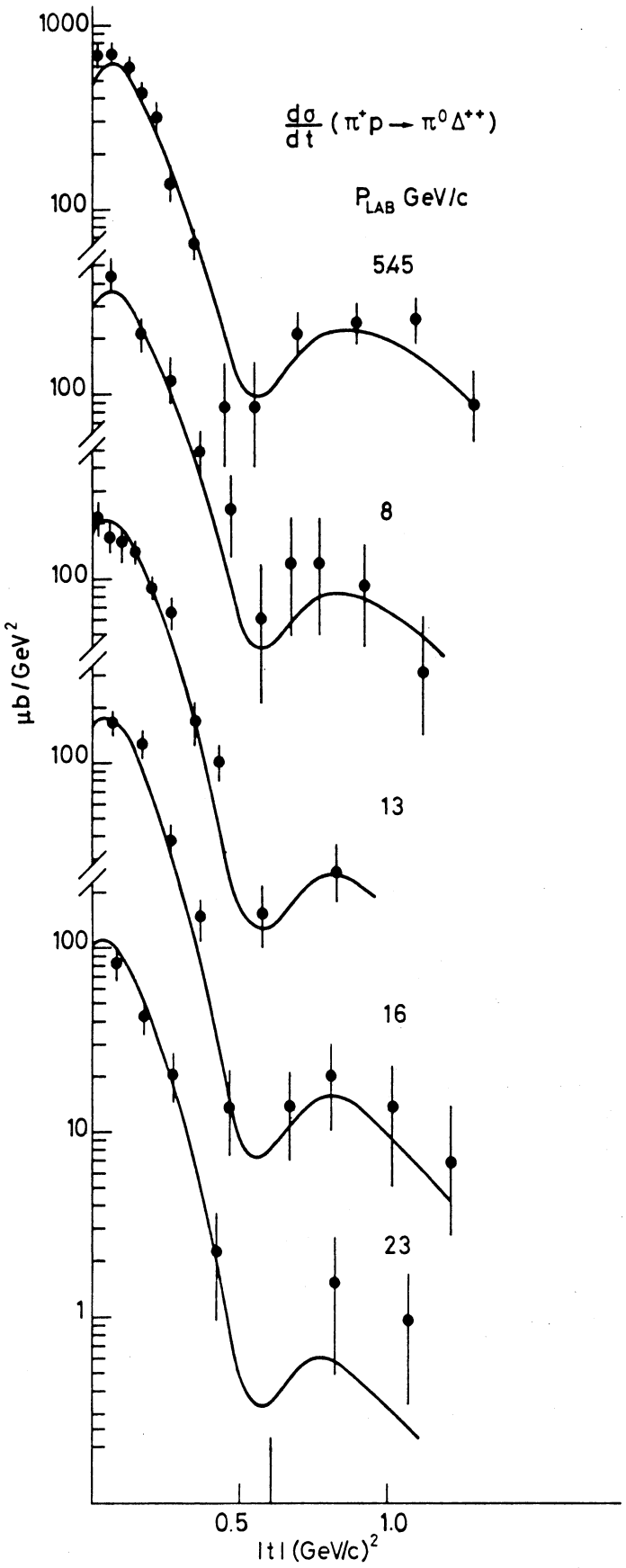
1000
100
100
100
100
100
10
1
$\frac{d\sigma}{dt}(\pi^+p \to \pi^0\Delta^{++})$
P_{LAB} GeV/c
5.45
8
13
16
23
μb/GeV²
0.5
1.0
|t| (GeV/c)²

FIG. 1

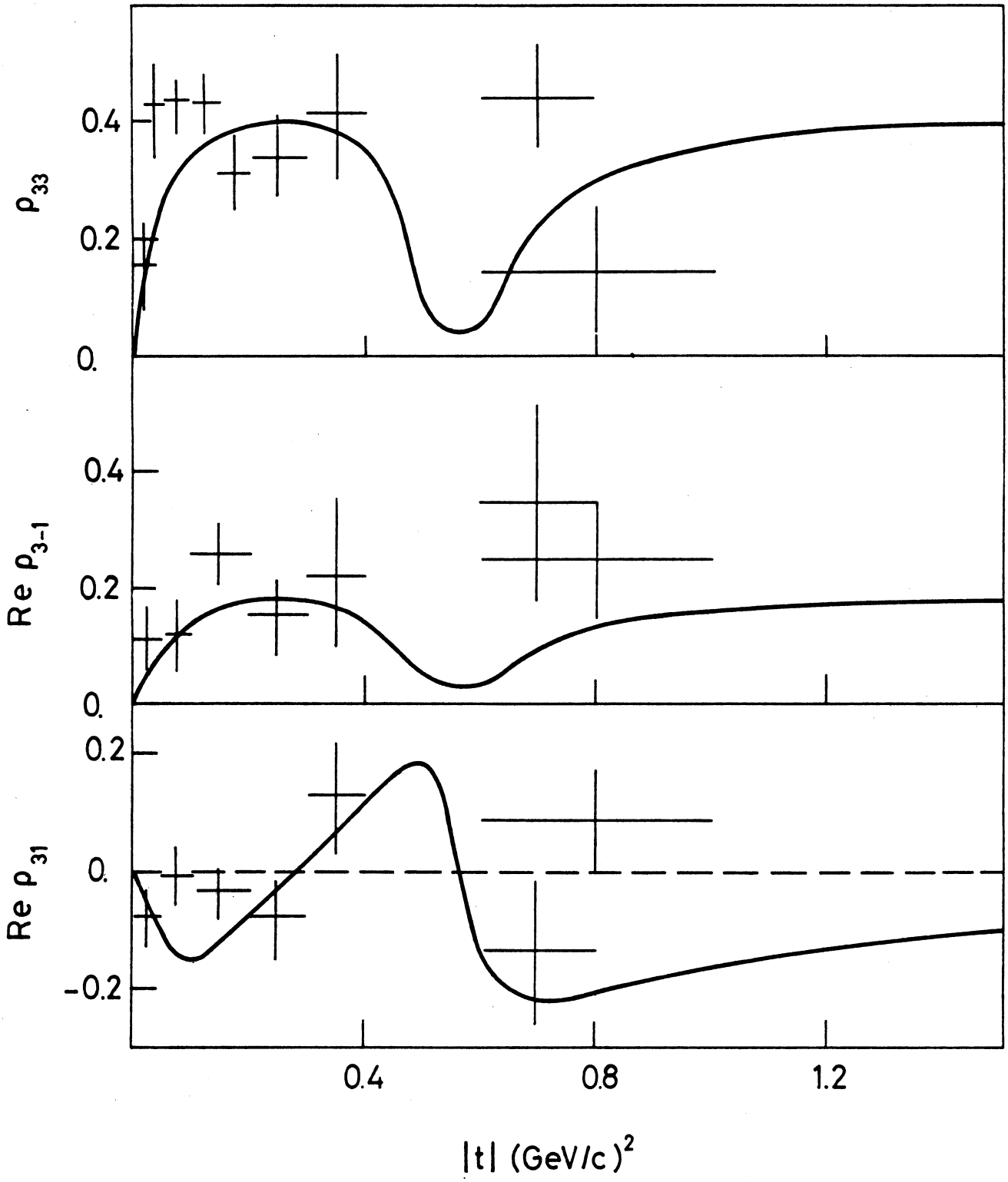

FIG. 2

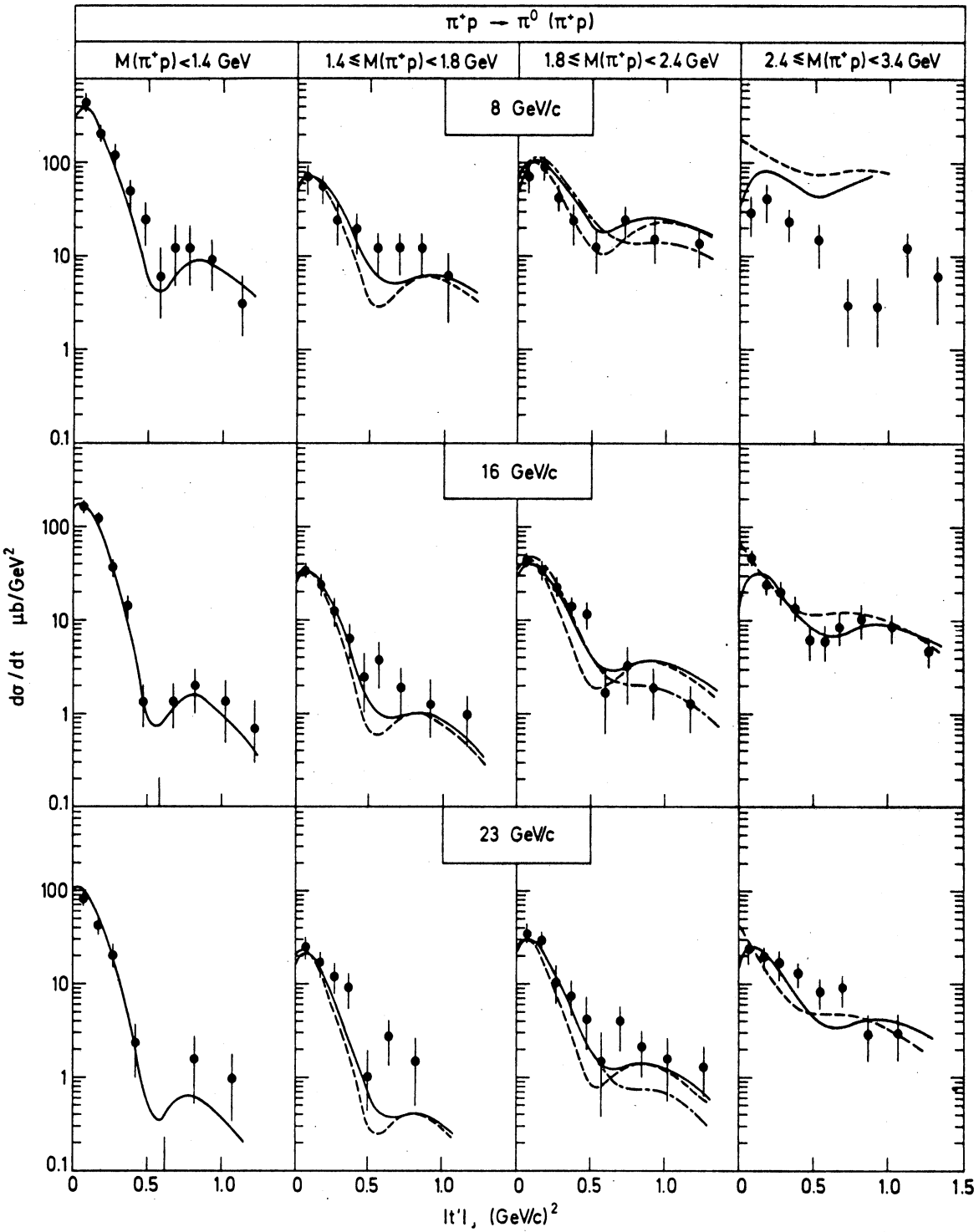
π⁺p → π⁰ (π⁺p)
M(π⁺p)<1.4 GeV
1.4≤M(π⁺p)<1.8 GeV
1.8≤M(π⁺p)<2.4 GeV
2.4≤M(π⁺p)<3.4 GeV
8 GeV/c
16 GeV/c
23 GeV/c
dσ/dt μb/GeV²
100
10
1
0.1
0
0.5
1.0
1.5
|t'|, (GeV/c)²

FIG. 3